Modelling of composite sandwich structures with honeycomb core subjected to high-velocity impact

Brenda L. Buitrago [a,b], Carlos Santiuste [a], Sonia Sánchez-Sáez [a], Enrique Barbero [a,*], Carlos Navarro [a]

[a] Department of Continuum Mechanics and Structural Analysis, University Carlos III of Madrid, Avda. de la Universidad 30, 28911 Leganés, Madrid, Spain
[b] Department of Industrial Technology, Simón Bolivar University, Valle de Sartenejas, Caracas, Venezuela

ARTICLE INFO

Keywords:
Sandwich structures
Numerical simulation
High-velocity impact
Honeycomb core

ABSTRACT

In this study the perforation of composite sandwich structures subjected to high velocity impact was analysed. Sandwich panels with carbon/epoxy skins and an aluminium honeycomb core were modelled by a three dimensional finite element model implemented in ABAQUS/Explicit. The model was validated with experimental tests by comparing numerical and experimental residual velocity, ballistic limit, and contact time. By this model the influence of the components on the behaviour of the sandwich panel under impact load was evaluated; also, the contribution of the failure mechanisms to the energy absorption of the projectile kinetic energy was determined.

1. Introduction

Sandwich structures are commonly used for weight efficient components in aerospace applications. The most usual components of aerospace sandwiches are carbon fibre skins and a honeycomb core due to their high specific stiffness and strength. During service, these structures may encounter high velocity impacts from low weight debris. Sandwich structures are very sensible to such loads. Despite extensive research on sandwich structures, their impact behaviour is still not fully understood [1].

The impact behaviour of a sandwich panel depends on many factors, not only the mechanical properties of its constituents, skins and core, but also the adhesive capacity of the skin core interface. This high velocity impact behaviour differs from the low velocity one, and therefore the conclusions drawn in studies on low velocity impacts are not applicable to high velocity cases. In this way, a high velocity impact is a phenomenon controlled by wave propagation, and is essentially independent of boundary conditions, whereas a low velocity impact is highly influenced by the boundary conditions.

Most studies on high velocity impact behaviour of sandwich structures are based on experimental tests [2,3]. Although experimental studies provide information on the sandwich structure tested, since impact phenomena depend on numerous parameters, knowledge of its influence on ballistic behaviour requires a broad test programme, which is time consuming and expensive. To reduce the cost and time, it is essential to use theoretical modelling.

The models most widely used to analyse the perforation of sandwich structures are analytical models [4] and numerical ones [5]. The main advantage of analytical models is the quick analysis of the influence of different parameters in the armour behaviour of the sandwich. However, with these simplified models, it is not possible to study in depth the perforation process of a sandwich panel.

To model the complete process of perforation, the behaviour both of the skins and the core need to be known. The behaviour of a carbon/epoxy composite skin can be considered lineal elastic until the laminate begins to fail. There are several failure mechanisms in a laminate: matrix cracking, tensile and compressive fibre breakage, delamination, etc., which depend of many parameters (e.g. fibre and matrix properties, characteristic of the fibre matrix interface, manufacturing process). The techniques to model the failure of laminates can be classified into three groups fracture mechanics, failure criteria, and damage mechanics although in some cases it is possible to combine some of them [6]. Of these, failure criteria have demonstrated to be valid in many studies, both under static and dynamic conditions. There are many different failure criteria in the literature [7]. Although some works apply simple failure criteria, such as Tsai Wu or Maximum Stress criteria to study the energy absorption characteristic of structural elements [8], it is necessary to consider all failure modes that can appear in the breakage of a laminate. Also the evolution of each failure mode and the relations among them has to be incorporated in the model [9]. Numerous failure criteria which consider several damage mechanisms have been used in the bibliography to analyse the failure of composite structures, such as the Hashin Rotem criteria [10], Chang Chang criteria [11], Puck criteria [12], Hou criteria [13] or Larc criteria [14].

* Corresponding author. Tel.: +34 91 624 99 65; fax: +34 91 624 94 30.
E-mail address: ebarbero@ing.uc3m.es (E. Barbero).

Nomenclature

1 2 3 axis	principal material coordinate system
E_1	lamina longitudinal modulus
E_2	lamina transverse modulus
E_{comp}	compressive modulus of the core
G_{12}	lamina shear modulus in the longitudinal and transverse plane
s	smooth parameter
S_{12}	shear strength in the longitudinal and transverse plane
S_{23}	shear strength in the transverse and normal plane
S_{31}	shear strength in the longitudinal and normal plane
X_t	tensile strength in longitudinal direction
X_c	compressive strength in longitudinal direction
Y_t	tensile strength in transverse direction
Y_c	compressive strength in transverse direction
Z_r	tensile strength in normal direction
ε_{11}	strain in the longitudinal direction
ε_{22}	strain in the transverse direction
ε_{33}	strain in the normal direction
ν_{12}	major Poisson ratio in the longitudinal and transverse plane
σ_{11}	stress in the longitudinal direction
σ_{22}	stress in the transverse direction
σ_{33}	stress in the normal direction
σ_{12}	shear stress in the longitudinal and transverse plane
σ_{23}	shear stress in the transverse and normal plane
σ_{31}	shear stress in the longitudinal and normal plane
σ_{ij}^{cor}	corrected stress
σ_{crush}	crush strength of the core
σ_{comp}	compressive strength of the core

The stress strain curve for the honeycomb core can be divided into three regions: firstly, linear elastic behaviour for low stress levels; secondly, when the stress reaches a certain level there is a region corresponding to progressive crushing at nearly constant stress level, and, finally a region of rapidly increasing stress due to the fact that the cell walls are closed [15]. Some authors analyse high velocity impact of sandwich panels using a model with an equivalent homogeneous material obtained by the experimental stress strain curve of the honeycomb [2]. However, in a high velocity impact the damage is concentrated around the impact point and thus differs from static crush behaviour, so that more advanced models become necessary. One possibility is to model each core cell with shell element, reproducing the real geometry Aktay et al. [16], Foo et al. [17]. Aktay et al. [16] analysed the crush behaviour of aluminium and NOMEX honeycomb using a FEM model under static conditions. Foo et al. [17] analysed the failure of sandwich panels with a three dimensional FEM model of the honeycomb core subjected to low velocity impact. Nia et al. [18] determined experimentally that the armour capacity of an aluminium honeycomb panel was small.

However, the influence of the honeycomb core inside a sandwich is not yet well known because there is a lack of studies on modelling the behaviour of honeycomb sandwich panels under high velocity impacts.

The influence of the honeycomb core on the stiffness and the strength of a sandwich panel under static or low velocity impacts has been widely studied, but few studies are available on the influence of the honeycomb core on the armour capacity of a sandwich panel, most being experimental studies.

In the present work, a numerical model is used to examine the behaviour of sandwich panels made of carbon/epoxy laminate skins with aluminium honeycomb core under high velocity impacts. The skins were modelled as laminates applying the Hou criteria [13] for the prediction of the failure, and the honeycomb core was modelled reproducing the aluminium hexagonal cells. The model was validated by experimental tests, and used to analyse the perforation procedure, evaluating the influence of the different components of a sandwich panel (skins and core) on the energy absorption process.

2. Material

In this work, square sandwich specimens (140 mm × 140 mm and 24 mm thick) were used. The skins were plain woven laminates of carbon fibres AS4 and epoxy resin 8552 and 2 mm in thickness. The core was a 3003 aluminium honeycomb of 20 mm thick and 77 kg/m^3 in density. The cells were hexagonal, with a size of4.8 mm a wall thickness of 60 μm.

The properties of the composite skins and the honeycomb core needed for the numerical model were determined by characterization tests. The properties of the carbon/epoxy woven laminate are shown in Table 1.

For the determination of the properties of the core, flat wise compression tests under square specimens were performed, according ASTM C 365/C365 M 05 Standard. An Instron 8516 servohydraulic machine was used with a loading rate of 0.5 mm/min. The load deflection curves were used to determine the compressive and crush strengths and the compressive modulus (Table 2).

3. Numerical model

The finite element model used to analyse the sandwich impact behaviour was implemented in ABAQUS/Explicit. Since the influence of boundary conditions is negligible in high velocity impacts, the FEM3D model included two solids: a projectile and a sandwich plate. Because no plastic deformation was found in the projectile after the experimental test, linear elastic behaviour was used for the steel projectile. The sandwich plate consisted of two materials: composite skins and an aluminium honeycomb core. The composite skins made up by a carbon fibre woven laminate were modelled using a VUMAT subroutine to define anisotropic mechanical properties and a set of failure criteria. The honeycomb core was divided into two regions; the zone close to the impact was modelled reproducing the aluminium hexagonal cells, while the distant zones were modelled by a homogeneous equivalent material.

3.1. Composite skins

In this work the composite failure criteria proposed by Hou was applied. These criteria include four failure modes: fibre failure, matrix cracking, matrix crushing, and delamination. The Hou model was developed to predict the failure of composite tape plies, in which the fibres are oriented in a single direction. A woven composite ply includes fibres at 0° and at 90° so that every ply has the same orientation. The matrix failure modes included in the Hou failure criteria considered that transverse loads are supported by the matrix. However, a woven laminate contains fibres in a transverse direction to support theses loads so that, in this analysis, the fibre failure criterion was applied to 0° and 90° directions [19]. The Brewer and Lagace [20] criterion was included in the subroutine formulation to predict delamination failure. Five failure

Table1
Mechanical properties of plain weave AS4/8552.

E_1 (GPa)	E_2 (GPa)	G_{12} (GPa)	ν_{12}	X_t (MPa)	X_c (MPa)	Y_t (MPa)	Y_c (MPa)	S_t (MPa)
68.5	68.5	3.7	0.11	795	860	795	860	98

Table 2
Mechanical properties of the honeycomb core.

σ_{comp} (MPa)	σ_{crush} (MPa)	E_{comp} (MPa)
3.76	1.8	400

criteria were evaluated: fibre failure, which considers tensile and compressive fibre failure in longitudinal and transverse directions, and delamination, which applies only to normal tensile stress.

2

$$d_{f1}^2 \quad \left(\frac{\sigma_{11}}{X_t}\right)^2 + \left(\frac{\sigma_{12}^2+\sigma_{13}^2}{S_{12}^2}\right) \quad \text{if } \sigma_{11} > 0 \tag{1}$$

$$d_{f1}^2 \quad \left(\frac{\sigma_{11}}{X_c}\right)^2 + \left(\frac{\sigma_{12}^2+\sigma_{13}^2}{S_{12}^2}\right) \quad \text{if } \sigma_{11} < 0 \tag{2}$$

$$d_{f2}^2 \quad \left(\frac{\sigma_{22}}{Y_t}\right)^2 + \left(\frac{\sigma_{12}^2+\sigma_{23}^2}{S_{12}^2}\right) \quad \text{if } \sigma_{22} > 0 \tag{3}$$

$$d_{f2}^2 \quad \left(\frac{\sigma_{22}}{Y_c}\right)^2 + \left(\frac{\sigma_{12}^2+\sigma_{23}^2}{S_{12}^2}\right) \quad \text{if } \sigma_{22} < 0 \tag{4}$$

$$d_{del}^2 \quad \left(\frac{\sigma_{33}}{Z_r}\right)^2 + \left(\frac{\sigma_{23}}{S_{23}}\right)^2 + \left(\frac{\sigma_{31}}{S_{31}}\right)^2 \quad \text{if } \sigma_{33} > 0 \tag{5}$$

Under a given load, the stresses at each integration point in the composite structure are computed in the material coordinate sys tem. Then, the stresses are substituted into the failure criteria. If any failure occurs, the material properties at that point are de graded according to the mode of failure. A fibre failure results in the complete failure of the material at that point, whereas a delam ination avoids only supporting stresses in a normal direction. In or der to degrade the material properties, the stresses in the damaged area were reduced close to zero according to which failure mode is verified (Table 3).

A sudden fall of mechanical properties involves instability prob lems and lack of convergence during simulation so that it is neces sary to develop a smooth transition between the stress values and zero. The stress components were corrected using the following equation:

$$\sigma_{ij}^{cor} \quad \sigma_{ij} \cdot \left(1 \quad \frac{2 \quad e^{S(d_i \ 0.5)}}{2 \quad e^{S/2}}\right) \tag{6}$$

As the projectile can perforate the composite skins during im pact, the model requires the use of a finite element erosion crite rion. The stresses on a finite element damaged drop to near zero while large deformations appear. These elements do not contribute to the stiffness or the strength of the plate, but they can cause instability problems. Maximum strain criteria were implemented in the VUMAT subroutine to remove the distorted elements: after each time increment the longitudinal strains (ε_{11}, ε_{22} and ε_{33}) are evaluated, and the element is removed if one of the strains reaches a critical value.

Table 3
Damage modes and corresponding stress update.

Damage mode	Stresses updated
Fibre failure	$\sigma_{11} = \sigma_{22} = \sigma_{33} = 0$ $\sigma_{12} = \sigma_{23} = \sigma_{13} = 0$
Delamination	$\sigma_{33} = \sigma_{23} = \sigma_{13} = 0$

3.2. Core

In a high velocity impact, the damage area is reduced to the re gion nearest the projectile trajectory. The honeycomb core model reproduces the geometry of the aluminium hexagonal cell in the region closest to the impact, considering the cell size, the film thickness, the density, and the compressive strength along the nor mal direction. In the numerical model, it was also considered that, due to the manufacturing process, some walls of the cell had dou ble thickness. The plastic behaviour of the 3003 aluminium alloy was implemented in a shell section. A numerical test was carried out over the honeycomb model to validate its compressive behav iour, comparing the results with the experimental flat wise com pression tests.

Since the damaged core was located in the region closed to the impact, the distant zones were modelled by a homogeneous aniso tropic equivalent material. The compressive behaviour of the equivalent material (Fig. 1), was estimated from the results of the experimental compression tests.

3.3. FEM3D model

Only a quarter of the panel was modelled due to the symmetry of the problem (Fig 2). A three dimensional non homogeneous mesh was used. Successive space discretizations were carried out to evaluate the sensitivity of the mesh. Finally, the selected mesh had 107,650 elements: 90,000 three dimensional 8 node brick ele ments with reduced integration (C3D8R in ABAQUS) in the com posite skins and the homogenous core, 17,300 two dimensional 4 node shell elements with reduced integration (S4R in ABAQUS) in the honeycomb core, and 350 three dimensional 4 node tetra hedral elements (C3D4 in ABAQUS) in the projectile. The woven

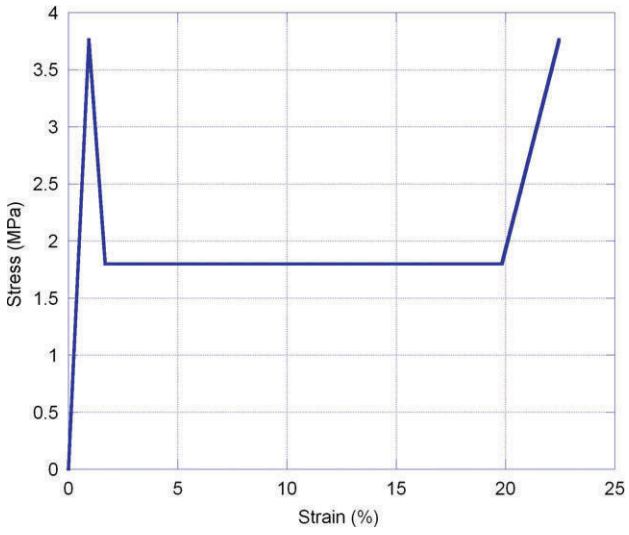

Fig. 1. Stress–strain curve of equivalent homogeneous core.

laminate consists of 10 elements along the thickness, one element per ply.

4. Experimental tests

To validate the numerical model, several high velocity impact tests were carried out on 25 specimens 140 mm in length, 140 mm in width, and 24 mm in thickness. These tests were per formed using an A1G + gas gun, manufactured by Sabre Ballistics. The specimens were impacted by spherical steel projectiles of 1.7 g and 7.5 mm in diameter. For a wide range of impact velocities from 92 m/s to 548 m/s, two different types of gases were used: helium to achieve the highest velocities, and Stargon® (a mixture of argon, carbon dioxide, and oxygen) for the lowest velocities. A high speed video camera was used (model ultima APX PHOTRON FASTCAM) to record the tests. This camera has a data acquisition system capable of taking up to 120,000 frames per second. For bet ter record quality, a high intensity light source, model ARRISUN 12 plus, was used. Information gathered from the tests was used to estimate the projectile velocity.

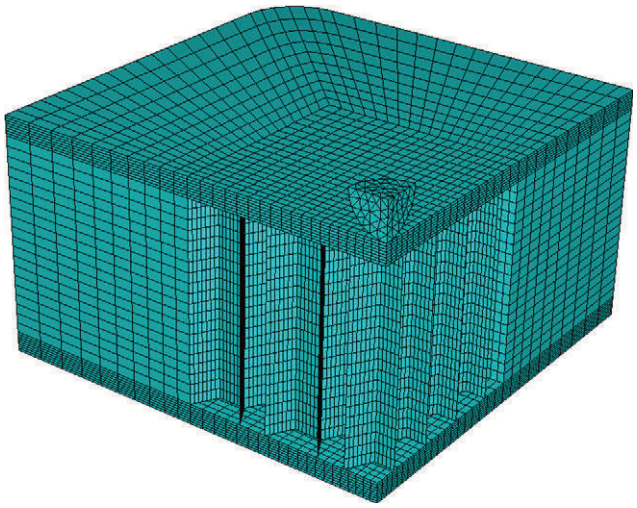

Fig. 2. Mesh used in the numerical model.

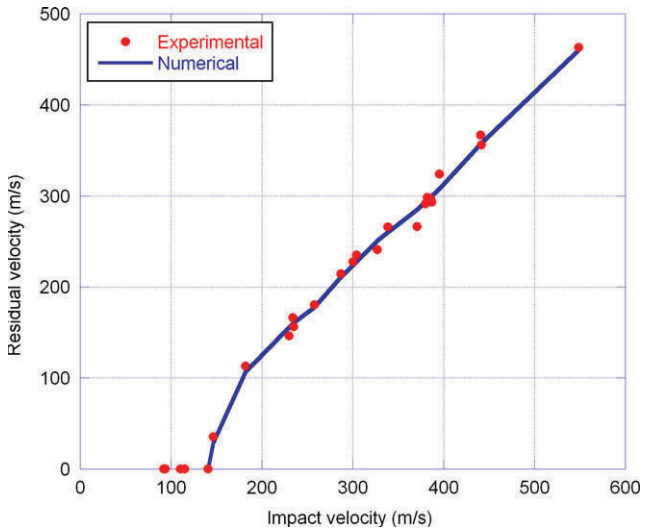

Fig. 3. Residual velocity versus impact velocity.

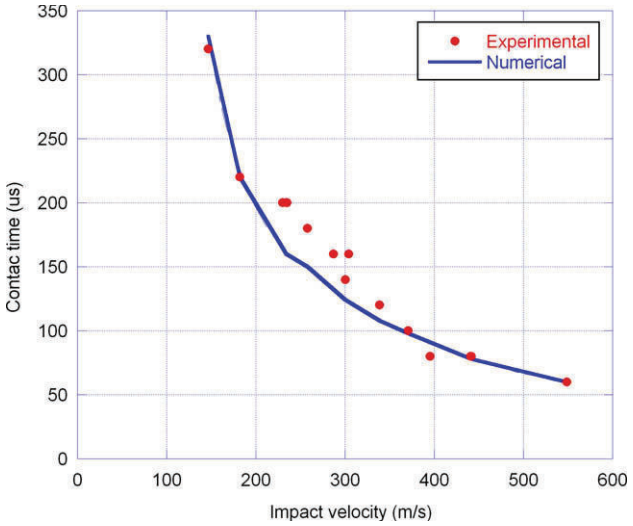

Fig. 4. Contact time versus impact velocity.

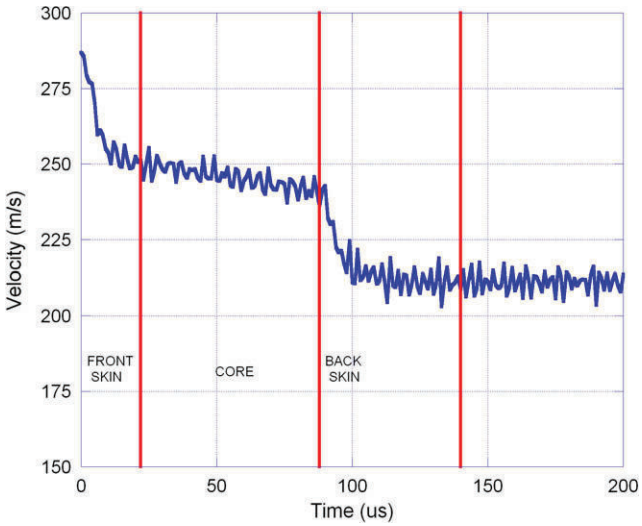

Fig. 5. Projectile velocity. Impact velocity = 287 m/s.

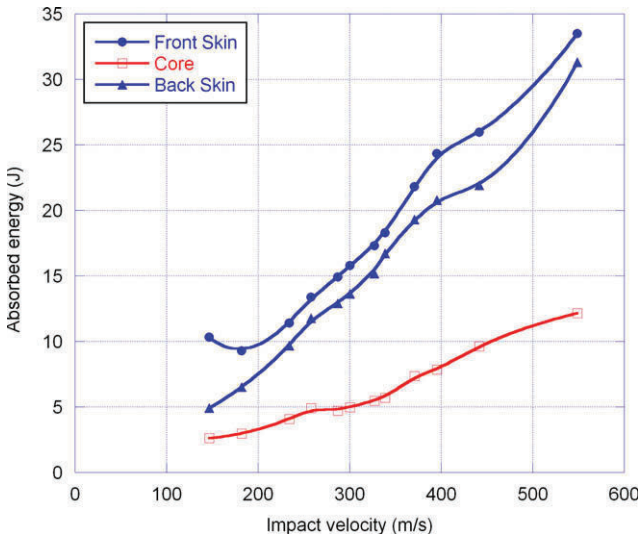

Fig. 6. Absorbed energy versus impact velocity.

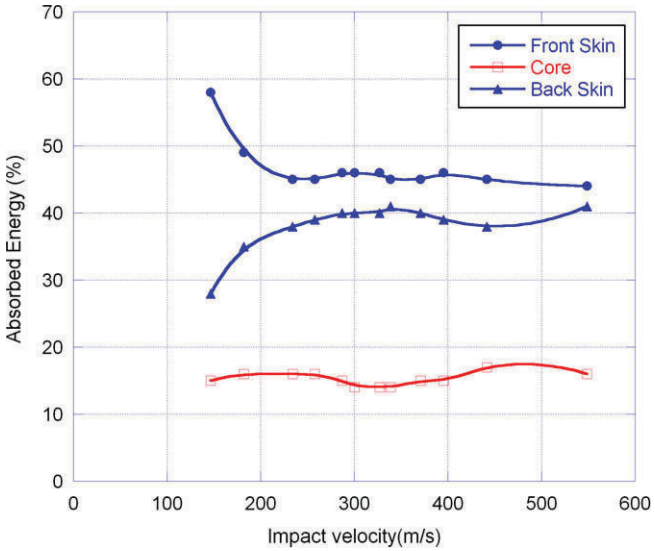

Fig. 7. Percentage of absorbed energy versus impact velocity.

5. Model validation

The numerical results were compared with the experimental ones to validate the finite element model. The variables selected to validate the numerical model were the residual velocity, the bal listic limit, and the contact time.

Fig. 3 shows experimental and numerical residual velocity as a function of the impact velocity. Numerical results were close to the experimental ones so that the precision of the model in the prediction of the residual velocity of the projectile was verified.

The ballistic limit was defined as the minimum impact velocity required for the projectile to completely penetrate the sandwich plate. From the model, the ballistic limit calculated was 142 m/s. The experimental ballistic limit estimated was 139 ± 4.2 m/s, by fitting the equation of Lambert and Jonas [21] to the residual veloc ity versus impact velocity curve. A comparison of the results from the numerical model and the experimental test gave a difference of 2% in the ballistic limit.

The contact time was estimated as the time between the con tact of the projectile with the front skin and the instant at which the projectile completely penetrated the sandwich plate. This

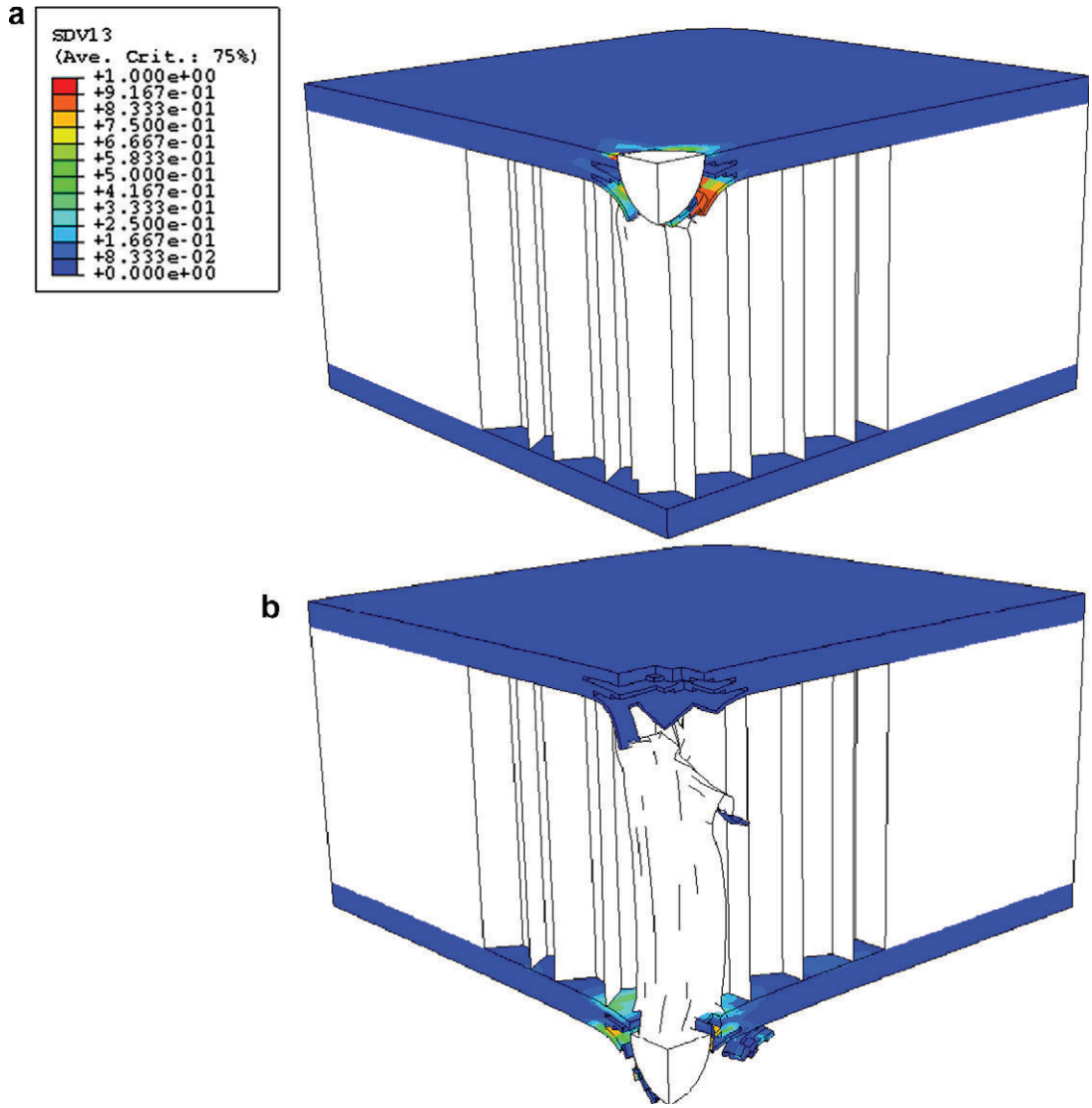

Fig. 8. Fibre-failure criterion during the sandwich perforation (impact velocity = 339 m/s). (a) t = 13 μs. (b) t = 105 μs.

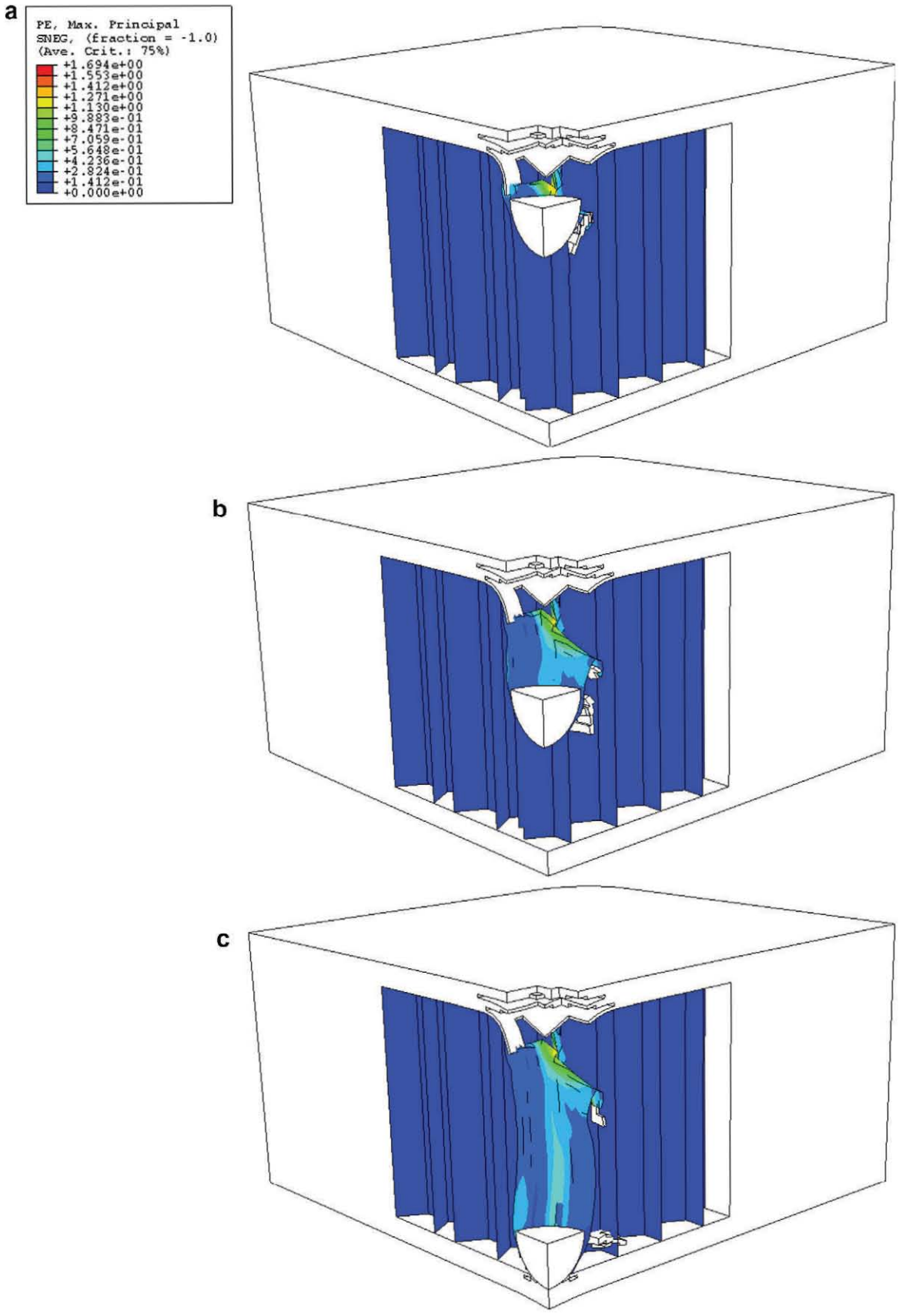

Fig. 9. Field of plastic strain during the sandwich perforation (impact velocity = 339 m/s). (a) t = 13 μs. (b) t = 51 μs. (c) t = 85 μs.

parameter also enabled validation of the numerical model, as a good correlation was found between the contact time measured experimentally and measured by the numerical model, as shown in Fig. 4.

6. Results

The drawback of the experimental impact tests is the limited information concerning the evolution of the projectile during the impact. The experimental tests provided information only about the velocity of the projectile before the impact over the front skin and after the perforation of the back skin. However, the finite ele ment model showed the evolution of the projectile while it was crossing through the sandwich plate. Fig. 5 shows the evolution of the projectile velocity during the impact (V_{imp} = 287 m/s).

The evolution of the velocity shown in Fig 5 is representative of each impact. There are three different trends corresponding to the three components of the sandwich (front skin, core, and back skin). In the first region (0 25 μs), the composite front skin caused a sud den drop in velocity at the beginning of the impact event, so that the projectile reached the honeycomb core at a velocity of nearly 250 m/s. Secondly (25 90 μs), the velocity remained almost con stant as the projectile went through the honeycomb core, when the projectile reached the back skin, its velocity was nearly 240 m/s. In the back skin (90 140 μs) a new drop in velocity was observed for a residual velocity of over 210 m/s. The projectile lost 46% of its impact kinetic energy, front and back skins absorbed 46% and 41% of the absorbed energy, respectively, and the honeycomb core absorbed 13%. This analysis was made on each numerical test, calculating the energy absorbed by the three components of the sandwich plate (Fig. 6).

The skins were the main factor responsible for the energy adsorption, while the energy absorbed by the honeycomb core was lower. The percentage of the energy absorbed by each compo nent was almost constant (Fig. 7) for impact velocities higher than 250 m/s: the front skin absorbed 45%, back skin 40%, and core 15% of the absorbed energy by the composite panel. However, when the impact velocity was near the ballistic limit, the front skin absorbed most of the impact energy so that the projectile reached the back skin at a low velocity. Thus, the energy absorbed by the back skin was reduced.

The use of the finite element model provides information about the failure modes in the perforation process. The main failure mode in the composite skins was fibre breakage. Fig. 8 shows the value of fibre failure criterion in composite skin during the impact. The energy absorption mechanism of the composite skins was based on fibre breakage. The energy needed to break high strength carbon fibres is very high, so the projectile underwent a sudden lost of kinetic energy when it penetrated a composite skin.

The main energy absorption mechanism of the honeycomb core was the plastic strain of the aluminium walls, Fig. 9. The energy needed to deform a thin walled cell of aluminium is very low, so the projectile crossed the honeycomb core with no major loss of ki netic energy. The experimental tests indicated that the region of the honeycomb over which the projectile impacted had no influ ence on the results. The numerical simulations showed similar re sults: impacts over the middle of the cell, over a wall of the cell, or over a junction of three walls, showed similar residual velocities.

7. Conclusions

In this study the perforation of composite sandwich panels subjected to high velocity impact was analysed using a three dimensional finite element model implemented in ABAQUS/Ex plicit. Experimental impact tests were carried out to validate the numerical model. Good agreement was found between numerical and experimental results; in particular, the numerical simulation was able to predict the ballistic limit of the sandwich panel with a difference of 2%.

The influence of both skins and the core in the energy absorp tion capabilities of the sandwich panel was studied in a broad range of impact velocities. Most of the impact energy was absorbed by the skins. For impact velocities above 250 m/s, approximately 45% of the impact energy was absorbed by the front skin and 40%by the back skin. For impact velocities close to ballistic limit, the front skin absorbed almost the 60% of the energy. On the con trary the honeycomb core absorbed between 10 and 20% of the im pact energy by plastic strain, at all the impact velocities analysed.

Also, the energy absorption mechanisms in both skins and the core were studied. The main mechanism in the skins was fibre breakage whereas in the core the mechanism was the plastic defor mation of the aluminium wall. Both in the skins and the core, the damage was concentrated in a small area around the impact point.

Acknowledgment

The authors are indebted to the Spanish Comisión Interministe rial de Ciencia y Tecnología (Project TRA2004 03960) for the finan cial support of this work.

References

[1] Aktay L, Johnson AF, Holzapfel M. Prediction of impact damage on sandwich composite panels. Comput Mater Sci 2005;32:252–60.
[2] Villanueva GR, Cantwell WJ. The high velocity impact response of composite and fml-reinforced sandwich structures. Compos Sci Technol 2004;64:35–54.
[3] Vaidya UK, Nelson S, Sinn B, Mathew B. Processing and high strain rate impact response of multi-functional sandwich composites. Compos Struct 2001;52:429–40.
[4] Ryan S, Schaefer F, Riedel W. Numerical simulation of hypervelocity impact on CFRP/Al HC SP spacecraft structures causing penetration and fragment ejection. Int J Impact Eng 2006;33:703–12.
[5] Icardi U, Ferrero L. Impact analysis of sandwich composites based on a refined plate element with strain energy updating. Compos Struct 2009;89:35–51.
[6] Allix O, Ladevéze P. Interlaminar interface modelling for the prediction of delamination. Compos Struct 1992;22:235–42.
[7] Paris F. A study of failure criteria of failure of fibrous composite materials. NASA/CR-2001-210661; 2001.
[8] Jadhav P, Mantena PR, Gibson RF. Energy absorption and damage evaluation of grid stiffened composite panels under transverse loading. Composites Part B 2006;37:191–9.
[9] Greve L, Pickett AK. Delamination testing and modelling for composite crash simulation. Compos Sci Technol 2006;66:816–26.
[10] Hashin Z, Rotem A. Fatigue criterion for fiber-reinforced materials. J Compos Mater 1973;7:448–64.
[11] Chang F, Chang K. A progressive damage model for laminated composites containing stress concentrations. J Compos Mater 1987;21:834–55.
[12] Puck A, Schurmann H. Failure analysis of FRP laminates by means of physically based phenomenological models. Compos Sci Technol 1998;58:1045–67.
[13] Hou JP, Petrinic N, Ruiz C, Hallett SR. Prediction of impact damage in composite plates. Compos Sci Technol 2000;60:273–81.
[14] Davila CG, Camanho PP. Failure criteria for FRP laminates in plane stress. NASA/RM-2003-212663; 2003.
[15] Meo M, Morris AJ, Vignjevic R, Marengo G. Numerical simulations of low-velocity impact on an aircraft sandwich panel. Compos Struct 2003;62:353–60.
[16] Aktay L, Johnson AF, Kroplin B-H. Numerical modelling of honeycomb core crush behaviour. Eng Fract Mech 2008;75:2616–30.
[17] Foo CC, Chai GB, Seah LK. A model to predict low-velocity impact response and damage in sandwich composites. Compos Sci Technol 2008;68:1348–56.
[18] Nia AA, Razavi SB, Majzoobi GH. Ballistic limit determination of aluminum honeycombs—experimental study. Mater Sci Eng A 2008;488:273–80.
[19] López-Puente J, Zaera R, Navarro C. Experimental and numerical analysis of normal and oblique ballistic impacts on thin carbon/epoxy woven laminates. Composites Part A 2008;39:374–87.
[20] Brewer JC, Lagace PA. Quadratic stress criterion for initiation of delamination. J Compos Mater 1988;22:1141–55.
[21] Lamber JP, Jonas GH. Toward standardization of in terminal ballistic testing: velocity representation. Report BRL-R-1852; 1976.